Articles

Construction of Metal Butterflies on a Metallacarborane Scaffold. 1. Synthesis and Structures of Bimetallic Precursors§

Thomas D. McGrath,* Shaowu Du, Bruce E. Hodson, Xiu Lian Lu, and F. Gordon A. Stone*

Department of Chemistry & Biochemistry, Baylor University, Waco, Texas 76798-7348

Received May 15, 2006

Treatment of $[N(PPh_3)_2][NEt_4][1,1,1\text{-}(CO)_3\text{-}2\text{-}Ph\text{-}closo\text{-}1,2\text{-}MCB_9H_9]$ (M = Mn (**1a**), Re (**1b**)) with sources of the cations $\{M'(CO)_2\}^+$ (M′ = Ir, Rh) affords the bimetallic species $[N(PPh_3)_2][1,3,6\text{-}\{M(CO)_3\}\text{-}3,6\text{-}(\mu\text{-}H)_2\text{-}1,1\text{-}(CO)_2\text{-}2\text{-}Ph\text{-}closo\text{-}1,2\text{-}M'CB_9H_7]$ (M = Re, M′ = Ir (**2a**), Rh (**2b**); M = Mn, M′ = Ir (**2c**), Rh (**2d**)). In these, the $\{M(CO)_3\}$ fragment, formerly a cluster vertex, has assumed an *exo*-polyhedral role, while the $\{M'(CO)_2\}$ units now occupy a site within the cluster. Compounds **2** convert to $[N(PPh_3)_2][1,3\text{-}\{M(CO)_4\}\text{-}3\text{-}(\mu\text{-}H)\text{-}1,1\text{-}(CO)_2\text{-}2\text{-}Ph\text{-}closo\text{-}1,2\text{-}M'CB_9H_8]$ (M = Re, M′ = Ir (**3a**), Rh (**3b**); M = Mn, M′ = Ir (**3c**), Rh (**3d**)) by deliberate CO addition or by CO scavenging. Reaction of **2b** with PEt_3 gives $[N(PPh_3)_2][1,3\text{-}\{Re(CO)_3(PEt_3)\}\text{-}3\text{-}(\mu\text{-}H)\text{-}1,1\text{-}(CO)_2\text{-}2\text{-}Ph\text{-}closo\text{-}1,2\text{-}RhCB_9H_8]$ (**4**), which has a mirror-symmetric structure, whereas **2a** with $NH_2C_6H_4Me$-1,4 affords $[N(PPh_3)_2][1,3\text{-}\{Re(CO)_3(NH_2C_6H_4Me\text{-}1,4)\}\text{-}3\text{-}(\mu\text{-}H)\text{-}1,1\text{-}(CO)_2\text{-}2\text{-}Ph\text{-}closo\text{-}1,2\text{-}IrCB_9H_8]$ (**5**), which is asymmetric. The structures of **2b**, **3b**, and **5** have been confirmed by X-ray diffraction studies.

Introduction

Metallacarborane complexes containing monocarbollide ligands, derived from monocarbon carboranes, often retain an overall anionic charge as a consequence of the high formal charge (typically 3−) on the carborane fragment.[1] While this feature may be useful in stabilizing the often unusual oxidation states accessible in such species,[2−4] its main utility lies in their reactions with electrophiles.[1] With H^+, for example, the metal center may simply be protonated to form a metal-hydride species,[5] or the proton may behave as a hydride abstractor and thereby facilitate substitution at a {BH} vertex.[1−3,6−11] Alternatively, when the electrophile is a cationic transition metal−ligand fragment, species containing multiple metal centers can result.[1,5a,9,10,12−20]

Among the latter class of reaction we have recently studied the reactivity of the dianionic, 11-vertex metallacarborane salts $[N(PPh_3)_2][NEt_4][1,1,1\text{-}(CO)_3\text{-}2\text{-}Ph\text{-}closo\text{-}1,2\text{-}MCB_9H_9]$ (M = Mn (**1a**),[4,19] Re (**1b**)[17]) (see Chart 1) and have demonstrated that both bi- and trimetallic products may be obtained by treatment with di- or monocationic metal fragments, respectively.[17−19] In particular, it was found that addition of a source of $\{Ir(CO)_2\}^+$ to **1b** afforded a bimetallic Ir−Re species that still carried a negative charge and hence could be treated with further cations (Scheme 1). Thus, with $\{Cu(PPh_3)\}^+$ two trimetallic products were obtained, whereas with $\{Au(PPh_3)\}^+$ only one trimetallic species was isolated, along with a tetrametallic cluster containing a "butterfly" configuration of metal atoms.[18] The species formed in this sequence were originally formulated as shown in Scheme 1. However, in elaborating upon these studies, it was revealed that one of our initial, very reasonable assump-

§ Dedicated to Professor Victor Riera, University of Oviedo, on the occasion of his 70th birthday.

* To whom correspondence should be addressed. E-mail: tom_mcgrath@baylor.edu; gordon_stone@baylor.edu.

(1) (a) McGrath, T. D.; Stone, F. G. A. *J. Organomet. Chem.* **2004**, *689*, 3891. (b) McGrath, T. D.; Stone, F. G. A. *Adv. Organomet. Chem.* **2005**, *53*, 1.

(2) Du, S.; Kautz, J. A.; McGrath, T. D.; Stone, F. G. A. *J. Chem. Soc., Dalton Trans.* **2001**, 2791.

(3) Du, S.; Kautz, J. A.; McGrath, T. D.; Stone, F. G. A. *Dalton Trans.* **2003**, 46.

(4) Du, S.; Farley, R. D.; Harvey, J. N.; Jeffery, J. C.; Kautz, J. A.; Maher, J. P.; McGrath, T. D.; Murphy, D. M.; Riis-Johannessen, T.; Stone, F. G. A. *Chem. Commun.* **2003**, 1846.

(5) (a) Batten, S. A.; Jeffery, J. C.; Jones, P. L.; Mullica, D. F.; Rudd, M. D.; Sappenfield, E. L.; Stone, F. G. A.; Wolf, A. *Inorg. Chem.* **1997**, *36*, 2570. (b) Blandford, I.; Jeffery, J. C.; Redfearn, H.; Rees, L. H.; Rudd, M. D.; Stone, F. G. A. *J. Chem. Soc., Dalton Trans.* **1998**, 1669.

(6) Ellis, D. D., Franken, A.; Jelliss, P. A.; Stone, F. G. A.; Yu, P.-Y. *Organometallics* **2000**, *19*, 1993.

(7) Franken, A.; Du, S.; Jelliss, P. A.; Kautz, J. A.; Stone, F. G. A. *Organometallics* **2001**, *20*, 1597.

(8) Du, S.; Franken, A.; Jelliss, P. A.; Kautz, J. A.; Stone, F. G. A.; Yu. P.-Y. *J. Chem. Soc., Dalton Trans.* **2001**, 1846.

(9) Kautz, J. A.; McGrath, T. D.; Stone, F. G. A. *Polyhedron* **2003**, *22*, 109.

(10) Franken, A.; McGrath, T. D.; Stone, F. G. A. *Organometallics* **2005**, *25*, 5157.

(11) McGrath, T. D.; Franken, A.; Kautz, J. A.; Stone, F. G. A. *Inorg. Chem.* **2005**, *44*, 8135.

(12) Blandford, I.; Jeffery, J. C.; Jelliss, P. A.; Stone, F. G. A. *Organometallics* **1998**, *17*, 1402.

(13) Jeffery, J. C.; Jelliss, P. A.; Rees, L. H.; Stone, F. G. A. *Organometallics* **1998**, *17*, 2258.

(14) Ellis, D. D.; Franken, A.; Stone, F. G. A. *Organometallics* **1999**, *18*, 2362.

(15) Ellis, D. D.; Franken, A.; Jelliss, P. A.; Kautz, J. A.; Stone, F. G. A.; Yu, P.-Y. *J. Chem. Soc., Dalton Trans.* **2000**, 2509.

(16) Du, S.; Kautz, J. A.; McGrath, T. D.; Stone, F. G. A. *Inorg. Chem.* **2003**, *40*, 6563.

(17) Du, S.; Kautz, J. A.; McGrath, T. D.; Stone, F. G. A. *Organometallics* **2003**, *22*, 2842.

(18) Du, S.; Kautz, J. A.; McGrath, T. D.; Stone, F. G. A. *Angew. Chem., Int. Ed.* **2003**, *42*, 5728.

(19) Du, S.; Jeffery, J. C.; Kautz, J. A.; Lu, X. L.; McGrath, T. D.; Miller, T. A.; Riis-Johannessen, T.; Stone, F. G. A. *Inorg. Chem.* **2005**, *44*, 2815.

(20) Lei, P.; McGrath, T. D.; Stone, F. G. A. *Chem. Commun.* **2005**, 3706.

10.1021/om060417z CCC: $33.50
Publication on Web 08/17/2006

Chart 1

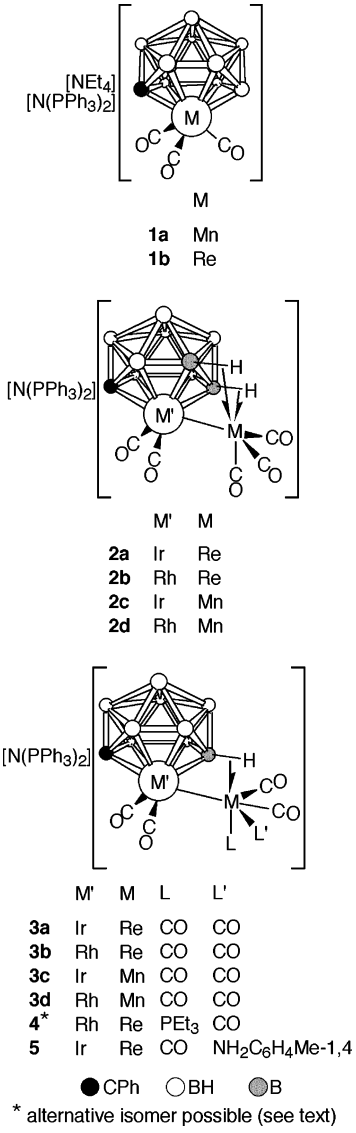

	M
1a	Mn
1b	Re

	M'	M
2a	Ir	Re
2b	Rh	Re
2c	Ir	Mn
2d	Rh	Mn

	M'	M	L	L'
3a	Ir	Re	CO	CO
3b	Rh	Re	CO	CO
3c	Ir	Mn	CO	CO
3d	Rh	Mn	CO	CO
4*	Rh	Re	PEt_3	CO
5	Ir	Re	CO	$NH_2C_6H_4Me$-1,4

* alternative isomer possible (see text)

Scheme 1. Original Formulations[18] of the Products Obtained from Sequential Reaction of 1b with $\{Ir(CO)_2\}^+$ and Then $\{Cu(PPh_3)\}^+$ or $\{Au(PPh_3)\}^{+a}$

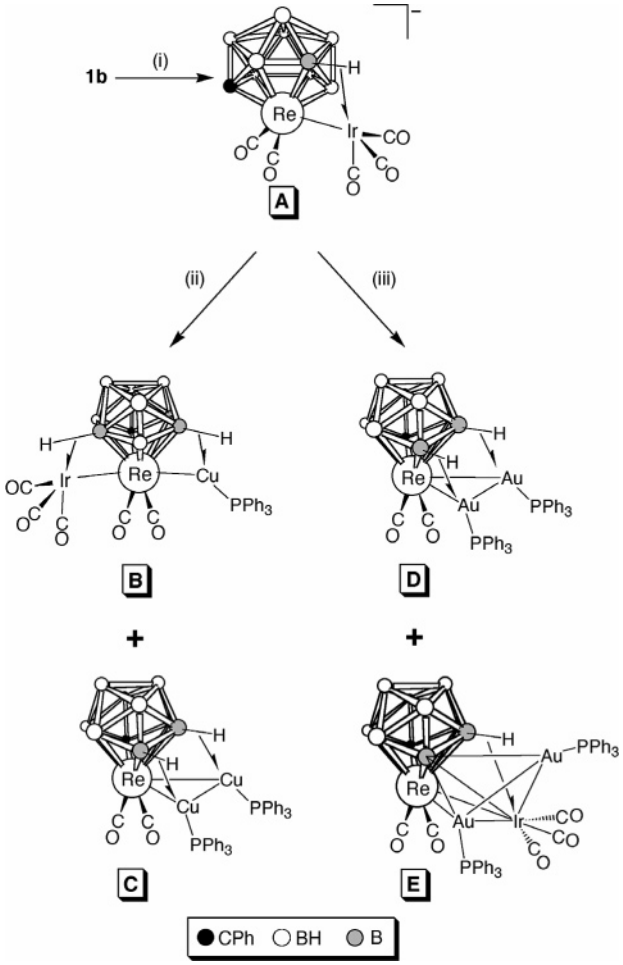

[a] Key: (i) $\{Ir(CO)_2\}^+$; (ii) $\{Cu(PPh_3)\}^+$; (iii) $\{Au(PPh_3)\}^+$.

tions was in fact erroneous. This led to a re-evaluation of this system and the discovery of metal atom site exchanges unprecedented in metallacarborane chemistry, upon which we now report.

Results and Discussion

Reaction of compounds **1** with sources of either $\{Ir(CO)_2\}^+$ or $\{Rh(CO)_2\}^+$ gives the salts $[N(PPh_3)_2][1,3,6\text{-}\{M(CO)_3\}\text{-}3,6\text{-}(\mu\text{-}H)_2\text{-}1,1\text{-}(CO)_2\text{-}2\text{-}Ph\text{-}closo\text{-}1,2\text{-}M'CB_9H_7]$ (M = Re, M′ = Ir (**2a**) or Rh (**2b**); M = Mn, M′ = Ir (**2c**) or Rh (**2d**)) (see Chart 1). Compound **2a** is that incorrectly formulated[18] as **A** in the initial work (see Scheme 1): It was very reasonably but erroneously assumed that the rhenium center in **1b** remained a cluster vertex upon conversion to **2a**. An X-ray diffraction study on **E** could only reveal an *apparent* transfer of one CO ligand from the cluster vertex to the *exo*-polyhedral metal−carbonyl fragment; very preliminary structural studies on **B** and **C** appeared also to confirm the CO transfer. This enigma highlights the difficulty in such experiments of distinguishing between pairs of atoms—in this case Re and Ir—that are close in atomic number.

No such ambiguity exists, however, in the cases of compounds **2b**−**2d**, and single-crystal X-ray analysis on **2b** confirmed the correct formulation shown in Chart 1. The structure of the anion of **2b** is shown in Figure 1. In this, the cluster metal vertex was definitively identified as being a rhodium center that bears two terminal CO ligands as in the source reagent $[Rh_2(\mu\text{-}Cl)_2(CO)_4]$, and the $\{Re(CO)_3\}$ unit was shown now to have assumed an *exo*-polyhedral site. The latter moiety is attached via a Rh−Re bond (Rh−Re is 2.8765(6) Å) and by two agostic-type B−H⇀Re interactions (B(3)···Re = 2.269(3), Re−H(3) = 2.03(3), B(6)···Re = 2.325(3), Re−H(6) = 2.03(3) Å). These three-center, two-electron bonds involve boron vertexes that are γ and β, respectively, with respect to the carbon atom in the rhodium-bound CB*BB*BB face. This mode of bonding to the cage for the *exo*-polyhedral $\{Re(CO)_3\}$ fragment in **2b** (and, by extension, for all of the *exo*-polyhedral units of compounds of type **2**) resembles that proposed[17,19] for the *exo*-$\{M(CO)_3\}$ derivatives (M = Mn, Re) of compounds **1**. Such a geometry was also observed recently in the molybdenacarborane derivatives $[1,3,6\text{-}\{Mo(CO)_3\}\text{-}3,6\text{-}(\mu\text{-}H)_2\text{-}1,1,1\text{-}(CO)_3\text{-}2\text{-}Ph\text{-}closo\text{-}1,2\text{-}MoCB_9H_7]^{3-}$ and $[1,3,6\text{-}\{Mn(CO)_3\}\text{-}3,6\text{-}(\mu\text{-}H)_2\text{-}1,1,1\text{-}(CO)_3\text{-}2\text{-}Ph\text{-}closo\text{-}1,2\text{-}MoCB_9H_7]^{2-}$ that are isolobal with compounds **2**.[20] Indeed, a brief consideration of the coordination geometry around the rhenium atom in **2b** shows that it is pseudo-octahedral, as is reasonable for the Re^I, d^6 metal center. This additionally confirms the metal atom assignments, as a Rh^I center, formally d^8, would not be expected to assume such octahedral coordination.

Table 1. Analytical and Physical Data

compd	color	yield/%	ν_{max}(CO)[a]/cm^{-1}	anal.[b] (%) C	H	N
[N(PPh$_3$)$_2$][1,3,6-{Re(CO)$_3$}-3,6-(μ-H)$_2$-1,1-(CO)$_2$-2-Ph-*closo*-1,2-IrCB$_9$H$_7$] (**2a**)	yellow	63	2048 s, 2011 s, 1985 s, 1915 br s	45.8 (46.0)	3.6 (3.5)	1.2 (1.1)
[N(PPh$_3$)$_2$][1,3,6-{Re(CO)$_3$}-3,6-(μ-H)$_2$-1,1-(CO)$_2$-2-Ph-*closo*-1,2-RhCB$_9$H$_7$] (**2b**)	orange	55	2056 s, 2011 vs, 1917 br vs	49.3 (49.6)	3.8 (3.8)	1.2 (1.2)
[N(PPh$_3$)$_2$][1,3,6-{Mn(CO)$_3$}-3,6-(μ-H)$_2$-1,1-(CO)$_2$-2-Ph-*closo*-1,2-IrCB$_9$H$_7$] (**2c**)	dark red	32	2049 s, 2003 vs, 1981 s, 1927 br s	52.2 (52.4)[c]	4.7 (4.4)	1.3 (1.2)
[N(PPh$_3$)$_2$][1,3,6-{Mn(CO)$_3$}-3,6-(μ-H)$_2$-1,1-(CO)$_2$-2-Ph-*closo*-1,2-RhCB$_9$H$_7$] (**2d**)	dark red-orange	32	2056 s, 2006 br s, 1928 br s	53.0 (52.7)[d]	4.3 (4.2)	1.3 (1.2)
[N(PPh$_3$)$_2$][1,3-{Re(CO)$_4$}-3-(μ-H)-1,1-(CO)$_2$-2-Ph-*closo*-1,2-IrCB$_9$H$_8$] (**3a**)	yellow	94	2096 s, 2029 s, 2007 vs, 1983 s, 1939 m	46.6 (47.0)[c]	3.7 (3.8)	1.1 (1.1)
[N(PPh$_3$)$_2$][1,3-{Re(CO)$_4$}-3-(μ-H)-1,1-(CO)$_2$-2-Ph-*closo*-1,2-RhCB$_9$H$_8$] (**3b**)	yellow	93	2094 s, 2041 s, 2014 vs, 1982 s, 1939 s	49.4 (49.2)	3.7 (3.4)	1.2 (1.2)
[N(PPh$_3$)$_2$][1,3-{Mn(CO)$_4$}-3-(μ-H)-1,1-(CO)$_2$-2-Ph-*closo*-1,2-IrCB$_9$H$_8$] (**3c**)	yellow	89	2081 s, 2024 s, 2005 vs, 1984 s, 1945 m	52.8 (53.1)[e]	4.8 (4.6)	1.2 (1.2)
[N(PPh$_3$)$_2$][1,3-{Mn(CO)$_4$}-3-(μ-H)-1,1-(CO)$_2$-2-Ph-*closo*-1,2-RhCB$_9$H$_8$] (**3d**)	yellow	88	2079 s, 2035 s, 2016 s, 1984 s, 1942 m	53.6 (53.9)[f]	4.3 (4.1)	1.3 (1.3)
[N(PPh$_3$)$_2$][1,3-{Re(CO)$_3$(PEt$_3$)}-3-(μ-H)-1,1-(CO)$_2$-2-Ph-*closo*-1,2-RhCB$_9$H$_8$] (**4**)	yellow	89	2049 s, 2011 s, 1995 s, 1924 vs, 1901 s	49.1 (49.4)[f]	4.5 (4.6)	1.0 (1.1)
[N(PPh$_3$)$_2$][1,3-{Re(CO)$_3$(NH$_2$C$_6$H$_4$Me-1,4)}-3-(μ-H)-1,1-(CO)$_2$-2-Ph-*closo*-1,2-IrCB$_9$H$_8$] (**5**)	pale yellow	79	2038 vs, 2007 s, 1974 s, 1912 br s	50.3 (50.0)[g]	4.1 (4.1)	2.1 (2.0)

[a] Measured in CH_2Cl_2; in addition, the spectra of all compounds show a broad, medium-intensity band ca. 2500−2550 cm^{-1} due to B−H absorptions. [b] Calculated values are given in parentheses. [c] Cocrystallized with 0.5 molar equiv of C_5H_{12}. [d] Cocrystallized with 1.0 molar equiv of CH_2Cl_2. [e] Cocrystallized with 1.0 molar equiv of C_5H_{12}. [f] Cocrystallized with 0.5 molar equiv of CH_2Cl_2. [g] Cocrystallized with 0.5 molar equiv of C_7H_8.

Spectroscopic data for all of compounds **2** are collected in Tables 1−3. Further evidence in support of the formulation of **2b** established in the X-ray study is provided by the $^{13}C\{^1H\}$ NMR spectrum (Table 2), which, crucially, shows five resonances for metal−carbonyl groups, of which only two show doublet structure due to coupling with a ^{103}Rh nucleus. Thus the metal center bearing only two CO ligands must be Rh, while that bearing three CO groups must be Re. The $^{13}C\{^1H\}$ NMR spectrum for the analogous compound **2d** unfortunately shows only two CO resonances, at δ 222.9 (broad) and 191.3 (^{103}Rh-coupled doublet). These are assigned to Mn- and Rh-bound groups, respectively, the broadening of the former being due to the quadrupolar ^{55}Mn nucleus and to fluxional processes such as "in place" rotation of the {Mn(CO)$_3$} fragment with respect to the cage.[17] The $^{13}C\{^1H\}$ NMR spectra of the corresponding iridium derivatives **2a** and **2c** are similar, but of course the presence of the iridium center does not here provide additional corroborative coupling information.

In the $^{11}B\{^1H\}$ NMR spectra of compounds **2** nine separate resonances are seen (with some coincidences), which is indicative of an asymmetric structure and is consistent with the structure observed in the solid state for **2b**. This confirms also that the *exo*-polyhedral fragment does not migrate over the cluster surface, a process that could otherwise cause the whole anion to appear mirror symmetric on the NMR time scale.[17] In their ^{1}H NMR spectra, all four of compounds **2** show two broad signals to relatively high field, some of which show quartet structure. These are in the region typical of B−H→M agostic-type interactions[21] and again are in agreement with the solid-state structure and with a lack of migration of the *exo*-polyhedral moiety.

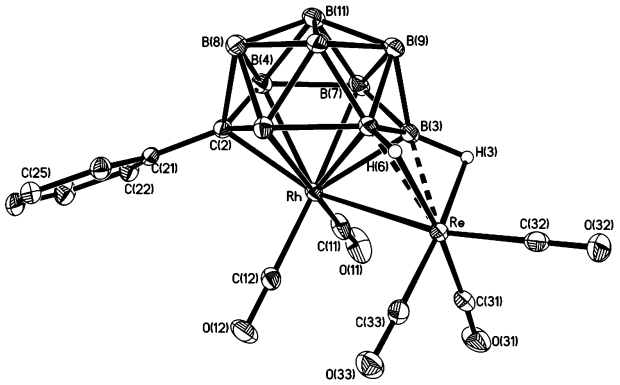

Figure 1. Structure of the anion of **2b** showing the crystallographic labeling scheme. In this and subsequent figures, thermal ellipsoids are shown at 40% probability and only chemically important H atoms are shown. Selected distances (Å) and angles (deg) are as follows: Rh−Re 2.8765(6), Rh−C(2) 2.167(3), Rh−B(3) 2.171(3), Rh−B(4) 2.436(3), Rh−B(5) 2.385(3), Rh−B(6) 2.384(3), Rh−B(7) 2.386(3), B(3)···Re 2.269(3), B(6)···Re 2.325(3); C(2)−Rh−Re 130.34(6), B(3)−Rh−Re 51.12(8), B(6)−Rh−Re 51.42(7).

Within compounds **2**, the dianionic irida- and rhodacarborane cores [1,1-(CO)$_2$-2-Ph-*closo*-1,2-M′CB$_9$H$_9$]$^{2-}$ (M′ = Ir, Rh) are themselves hitherto unknown. In principle, they ought to be accessible by means analogous to the synthesis of compounds **1**,[4,17,19] namely, treatment of the putative trianion [6-Ph-*nido*-6-CB$_9$H$_9$]$^{3-}$ with a source of {M′(CO)$_2$}$^+$, but in practice they have thus far proved elusive. In addition, the mechanism by which the {M(CO)$_3$} vertex (M = Re, Mn) is expelled from the cluster, and the {M′(CO)$_2$} unit assumes the vacated site, is also not clear. In related chemistry, we have shown[19] that the {Pt(dppe)}$^{2+}$ derivative of the anion of **1a** (structure **F** in Scheme 2; dppe = Ph$_2$PCH$_2$CH$_2$PPh$_2$) can rearrange to an isomeric 12-vertex platinamanganacarborane with a closed {PtMnCB$_9$} core (**G**) and that this can in turn eject a manganese unit to form a proposed {PtCB$_9$} cluster bearing an *exo*-polyhedral {Mn(CO)$_3$} moiety (structure **H**). In practice, the identity of **H** is somewhat speculative, as this species further loses a {BH} vertex to afford the observed final product **J**, where the {Mn(CO)$_3$} group is appended to a {PtCB$_8$} cluster. By analogy with this, we might propose that compounds **1** upon reaction with the cations {M′(CO)$_2$}$^+$ form a transient intermediate **K** (Scheme 2), which rearranges to the 12-vertex dimetallacarborane cluster **L**, and thence extrusion of the {M(CO)$_3$} fragment gives the observed 11-vertex anions of compounds **2** (structure **M**). As in that earlier study, it is not clear why (or how) the initial rearrangement **K** → **L** (or **F** → **G**) takes place. However, some observations reported and discussed in the following paper[22] may shed some light on this

(21) Brew, S. A.; Stone, F. G. A. *Adv. Organomet. Chem.* **1993**, *35*, 135.

Table 2. ^{1}H and ^{13}C NMR Data[a]

compd	^{1}H (δ)[b]	^{13}C (δ)[c]
2a	7.90 (m, 2H, cage-C$_6H_5$), 7.69−7.46 (m, 30H, PPh), 7.25 (m, 2H, cage-C$_6H_5$), 7.11 (m, 1H, cage-C$_6H_5$), −4.45 (br q, J(BH) ≈ 130, 1H, B−H⇀Re), ca. −7.9 (vbr, 1H, B−H⇀Re)	197.7 (Re−CO), 173.1 (br, Ir−CO), 149.7, 134.1−125.6 (Ph), 56.8 (br, cage C)
2b	7.87 (m, 2H, cage-C$_6H_5$), 7.70−7.45 (m, 30H, PPh), 7.24 (m, 2H, cage-C$_6H_5$), 7.10 (m, 1H, cage-C$_6H_5$), −3.85 (br q, J(BH) ≈ 110, 1H, B−H⇀Re), −7.27 (br q, J(BH) ≈ 90, 1H, B−H⇀Re)	198.9, 198.4, 195.0 (Re−CO × 3), 191.1 (d, J(RhC) = 85, Rh−CO), 190.3 (d, J(RhC) = 67, Rh−CO), 150.5, 134.1−125.1 (Ph), 70.3 (br, cage C)
2c	7.90 (br m, 2H, cage-C$_6H_5$), 7.65−7.46 (br m, 30H, PPh), 7.24 (br m, 2H, cage-C$_6H_5$), 7.11 (m, 1H, cage-C$_6H_5$), ca. −5.7 (vbr q, J(BH) ≈ 110, 1H, B−H⇀Mn), ca. −9.1 (vbr, 1H, B−H⇀Mn)	226.6 (br, Mn−CO), 173.6 (Ir−CO), 150.0, 134.7−125.0 (Ph), 55.2 (br, cage C)
2d	7.90 (br m, 2H, cage-C$_6H_5$), 7.65−7.46 (br m, 30H, PPh), 7.23 (br m, 2H, cage-C$_6H_5$), 7.10 (m, 1H, cage-C$_6H_5$), ca. −5.5 (vbr q, J(BH) ≈110, 1H, B−H⇀Mn), ca. −8.9 (vbr q, 1H, J(BH) ≈ 105, 1H, B−H⇀Mn)	222.9 (br, Mn−CO), 191.3 (d, J(RhC) = 63, Rh−CO), 151.1, 134.1−125.2 (Ph), ca. 58.5 (vbr, cage C)
3a	7.84 (m, 2H, cage-C$_6H_5$), 7.71−7.44 (m, 30H, PPh), 7.25 (m, 2H, cage-C$_6H_5$), 7.11 (m, 1H, cage-C$_6H_5$), −7.91 (vbr q, J(BH) ≈ 100, 1H, B−H⇀Re)	191.6 (Re−CO), 190.2 (Re−CO × 2), 186.8 (Re−CO), 170.6 (Ir−CO × 2), 150.9, 134.6−125.3 (Ph), ca. 59.4 (br, cage C)
3b	7.93 (m, 2H, cage-C$_6H_5$), 7.67−7.44 (m, 30H, PPh), 7.24 (m, 2H, cage-C$_6H_5$), 7.07 (m, 1H, cage-C$_6H_5$), −7.59 (br q, J(BH) ≈ 100, 1H, B−H⇀Re)	193.0 (Re−CO), 191.7 (Re−CO × 2), 188.6 (d, J(RhC) = 59, Rh−CO × 2), 186.3 (Re−CO), 151.1, 134.1−125.1 (Ph), ca. 59.6 (vbr, cage C)
3c	7.93 (br m, 2H, cage-C$_6H_5$), 7.68−7.45 (br m, 30H, PPh), 7.25 (br m, 2H, cage-C$_6H_5$), 7.12 (br m, 1H, cage-C$_6H_5$), −10.71 (br q, J(BH) ≈ 100, 1H, B−H⇀Mn)	217.2 (br, Mn−CO), 171.5 (Ir−CO), 150.7, 134.9−125.4 (Ph), 61.7 (vbr, cage C)
3d	7.94 (br m, 2H, cage-C$_6H_5$), 7.66−7.46 (br m, 30H, PPh), 7.25 (br m, 2H, cage-C$_6H_5$), 7.11 (br m, 1H, cage-C$_6H_5$), −10.61 (br q, J(BH) ≈ 100, 1H, B−H⇀Mn))	217.9 (br, Mn−CO), 189.7 (d, J(RhC) = 60, Rh−CO), 150.8, 134.1−125.2 (Ph), 63.4 (vbr, cage C)
4	7.92 (m, 2H, cage-C$_6H_5$), 7.66−7.44 (m, 30H, PPh), 7.21 (m, 2H, cage-C$_6H_5$), 7.03 (m, 1H, cage-C$_6H_5$), 2.13 (dq, J(PH) = J(HH) = 8, 6H, PCH$_2$), 1.21 (dt, J(PH) = 16, 9H, PCH$_2$CH_3), −7.37 (br q, J(BH) ≈ 95, 1H, B−H⇀Re)	201.7 (Re−CO), 199.3 (d, J(PC) = 7, Re−CO × 2), 189.7 (d, J(RhC) = 60, Rh−CO × 2), 152.6, 134.1−124.4 (Ph), ca. 59.3 (vbr, cage C), 24.7 (d, J(PC) = 24, PCH$_2$), 8.6 (br, PCH$_2$CH$_3$)
5	7.91 (m, 2H, cage-C$_6H_5$), 7.69−7.46 (m, 30H, PPh), 7.25 (m, 2H, cage-C$_6H_5$), 7.16 (m, 2H, C$_6$H$_4$), 7.13 (m, 3H, cage-C$_6H_5$ and C$_6$H$_4$), 5.42 (br d, J(HH) ≈ 11, 1H, NH), 4.41 (br d, 1H, NH), 2.34 (s, 3H, Me), ca. −5.04 (vbr q, J(BH) ≈ 120, B−H⇀Re)	199.0, 195.5, 192.9 (Re−CO), 173.4, 170.5 (Ir−CO), 151.4, 144.7, 135.6−125.0, 119.7 (Ph and C$_6$H$_4$), 51.2 (vbr, cage C), 20.8 (Me)

[a] Chemical shifts (δ) in ppm, coupling constants (J) in Hz, measurements at ambient temperatures, except where indicated, in CD_2Cl_2. [b] Resonances for terminal BH protons occur as broad unresolved signals in the range δ ca. −1 to +3. [c] ^{1}H-decoupled chemical shifts are positive to high frequency of $SiMe_4$.

Scheme 2. Proposed Mechanism for the Formation of Compounds 2: *exo* ↔ *endo* Metal Fragment Site Exchange via a 12-Vertex Intermediate and, for Comparison, a Related Process in a Platinum−Manganese−Monocarbollide System (M = Re, Mn; M′ = Ir, Rh)

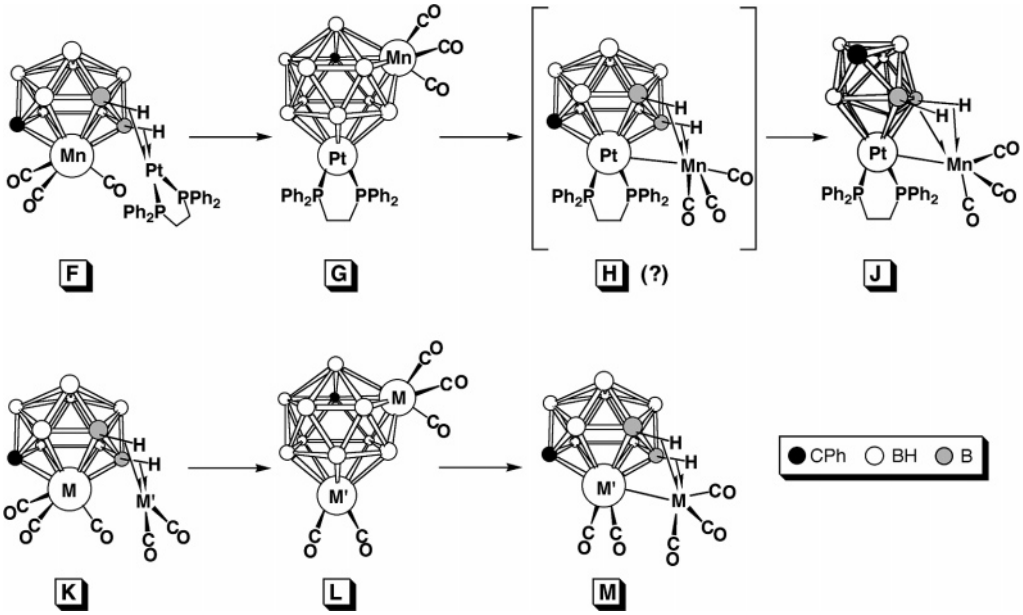

enigma. It also remains to be understood why the {metal−dicarbonyl} fragments apparently are preferred over {metal−tricarbonyl} groups as cluster vertexes, particularly given the hexahapticity of the {*nido*-CB$_9$} ligand.

There are a few other examples in the literature of carborane "cage transfer" from one metal center to another: the *endo*-{Au(PPh$_3$)}$^+$ derivative of [7,8-Me$_2$-*nido*-7,8-C$_2$B$_9$H$_9$]$^{2-}$ has been shown to transfer its carborane ligand to rhodium and iridium centers, with the gold fragment itself becoming *exo*-polyhedral.[23] In these cases, however, the *endo*-polyhedral {Au-

(22) McGrath, T. D.; Du, S.; Hodson, B. E.; Stone, F. G. A. *Organometallics* **2006**, *25*, 4452.

Table 3. ^{11}B and ^{31}P NMR Data[a]

compd	^{11}B (δ)[b]
2a	23.1, 16.1, 4.2, −6.2, −16.4, −18.6, −22.8, −24.0, −35.8
2b	29.6, 17.1, 3.6, −1.6, −12.8 (3B), −21.5, −32.9
2c	27.2, 17.1, 3.4, −6.8, −20.9 (2B), −21.4 (2B), −33.8 (br)
2d	34.0, 18.5, 2.6, −0.1, −12.0 (2B), −14.5, −22.2, −32.4
3a	50.8, 11.0, −7.6 (2B), −10.2, −23.1 (2B), −28.4 (2B)
3b	63.2, 12.9, −3.2 (2B), −10.9, −16.1 (2B), −25.4 (2B)
3c	56.9, 12.0, −6.9 (2B), −11.3, −23.3 (2B), −28.6 (2B)
3d	70.0, 14.1, −2.4 (2B), −12.0, −16.4 (2B), −25.6 (2B)
4[c]	65.4, 12.0, −4.3 (2B), −12.1, −17.1 (2B), −26.4 (2B)
5	51.5, 11.3, ca. −7.8 (br sh, 2B), −8.9 (br), −24.6, −28.6, −29.9 (2B)

[a] Chemical shifts (δ) in ppm, coupling constants (J) in Hz, measurements at ambient temperatures in CD_2Cl_2. [b] ^{1}H-decoupled chemical shifts are positive to high frequency of $BF_3{\cdot}Et_2O$ (external); resonances are of unit integral except where indicated, and where peaks are broad, the assigned integrals may be somewhat subjective. [c] ^{31}P{^{1}H} NMR (positive to high frequency of external 85% H_3PO_4): δ 11.4.

$(PPh_3)\}^+$ moiety is generally not considered to be a cluster vertex but a pseudo-proton,[24] and therefore its displacement from the *endo*-polyhedral cluster site is less surprising than in the present system. However, a more recent example involves the 13-vertex rhenacaborane anion [4,4,4-$(CO)_3$-*closo*-4,1,6-$ReC_2B_{10}H_{12}]^-$. This species apparently transfers its carborane ligand to a copper center in the formation of [4-PPh_3-4,7,10-{Cu(PPh_3)}-7,10-(μ-H)$_2$-*closo*-4,1,6-$CuC_2B_{10}H_{10}$], perhaps via a process that is akin to the formation of the compounds **2** from compounds **1**.[25]

All of compounds **2** are unstable in solution, with the rhodacarborane species being less stable than their iridium analogues, and with manganese-containing complexes being significantly less stable than the corresponding rhenium-containing ones. In all cases they appear to decompose with CO scavenging, and the process gives only a single identifiable metallacarborane product, namely, $[N(PPh_3)_2][1,3\text{-}\{M(CO)_4\}\text{-}3\text{-}(\mu\text{-H})\text{-}1,1\text{-}(CO)_2\text{-}2\text{-Ph-}closo\text{-}1,2\text{-M}'CB_9H_8]$ (M = Re, M′ = Ir (**3a**) or Rh (**3b**); M = Mn, M′ = Ir (**3c**) or Rh (**3d**)) (see Chart 1). At room temperature compounds **2a** and **2b** are converted to **3a** and **3b** only after many ($\geq$10−15) days, while compounds **2c** and **2d** can transform to **3c** and **3d** within a few (1−3) days. Indeed, whereas the former pair show only traces of the decomposition product (^{11}B NMR analysis) after 16 h at room temperature, the latter pair might show up to 50% conversion after this time. This process also appears to be very significantly accelerated by the presence of impurities. Thus, the conversion **2d** → **3d** is almost complete after ca. 16 h in CH_2Cl_2 solution at −30 °C when the compound is impure, but a pure sample under the same conditions survives with only ca. 50% decomposition after one month. These observations notwithstanding, compounds **2** can be converted more easily and almost quantitatively to compounds **3** by straightforward treatment of CH_2Cl_2 solutions of the former with a stream of CO, suggesting that the CO scavenging occurs *after* the decomposition rather than promoting that process.

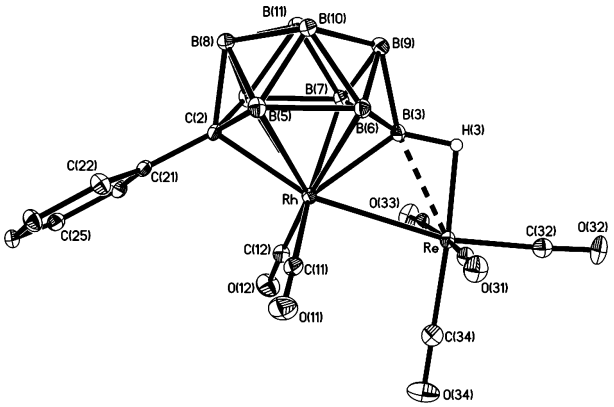

Figure 2. Structure of the anion of **3b** showing the crystallographic labeling scheme. Selected distances (Å) and angles (deg) are as follows: Rh−Re 2.8640(5), Rh−C(2) 2.184(2), Rh−B(3) 2.093(2), Rh−B(4) 2.508(3), Rh−B(5) 2.457(2), Rh−B(6) 2.346(2), Rh−B(7) 2.378(3), B(3)···Re 2.330(2); C(2)−Rh−Re 163.49(5), B(3)−Rh−Re 53.37(7).

Compounds **3** were characterized by X-ray diffraction studies and by the data presented in Tables 1−3 as described later. All four species gave crystals suitable for X-ray analysis, and of these the structure of the anion of **3b** is shown in Figure 2. The structures determined for **3a**, **3c**, and **3d** are very similar to that of **3b**—although of somewhat inferior quality—and are included as electronic Supporting Information only. In particular, it is noted that the structural analyses for the two manganese species **3c** and **3d** do serve to confirm unequivocally that the *exo*-polyhedral moiety in those complexes is an $\{Mn(CO)_4\}$ fragment. The structure determined for **3b** shows that, similar to **2b**, the *exo*-polyhedral $\{Re(CO)_4\}$ fragment is attached to the cluster surface via a direct Re−Rh bond: Rh−Re is 2.8640(5) Å, slightly shorter than in **2b**. In addition to the four carbonyl groups and the metal−metal bond, the pseudo-octahedral coordination around the rhenium is completed by a single B−H⇀Re interaction (B(3)···Re = 2.330(2), Re−H(3) = 1.85(2) Å). The latter now involves only the γ-BH unit in the Rh-bound CBB*B*BB belt. Overall the anion of **3b** is approximately mirror symmetric.

This symmetry is also evident in the ^{11}B{^{1}H} NMR spectra of all of compounds **3**. All four give rise to a set of six resonances in the integral ratio 1:1:2:1:2:2, consistent with time-averaged C_s symmetry in solution. Likewise, in their ^{1}H NMR spectra, only a single broad quartet resonance is seen for the sole B−H⇀M interaction in each species, at δ −7.91 (**3a**), −7.59 (**3b**), −10.71 (**3c**), and −10.61 (**3d**). As expected, the ^{13}C{^{1}H} NMR spectra of compounds **3a** and **3b** show three resonances in the apparent ratio 1:2:1 for the Re-bound CO ligands, plus a single resonance of relative intensity 2 (with typical $J(^{103}Rh^{13}C)$ coupling for **3b**) due to the $\{M'(CO)_2\}$ moieties. These correspond with a mirror symmetric structure (as observed for **3b** in the solid state) and with the *exo*-polyhedral $\{Re(CO)_4\}$ fragment being static in solution at ambient temperature. Similar to compounds **2c** and **2d**, the $\{Mn(CO)_4\}$ units in **3c** and **3d** give rise to only one broad peak in their ^{13}C{^{1}H} NMR spectra, while the $\{M'(CO)_2\}$ units resemble those in **3a** and **3b**, respectively. The chemical shifts and relative intensities of the CO resonances (definitively identified by their doublet structure when M′ = Rh) further corroborate the metal atom assignments in the solid state. We note again that all of this is consistent with the *exo* ↔ *endo* metal fragment site

(23) (a) Howard, J. A. K.; Jeffery, J. C.; Jelliss, P. A.; Sommerfeld, T.; Stone, F. G. A. *J. Chem. Soc., Chem. Commun.* **1991**, 1664. (b) Jeffery, J. C.; Jelliss, P. A.; Stone, F. G. A. *J. Chem. Soc., Dalton Trans.* **1993**, 1073. (c) Jeffery, J. C.; Jelliss, P. A.; Stone, F. G. A. *J. Chem. Soc., Dalton Trans.* **1993**, 1083. See also: Jeffery, J. C.; Jelliss, P. A.; Stone, F. G. A. *Organometallics* **1994**, *13*, 2651.

(24) See, for example: Macgregor, S. A.; Wynd, A. J.; Moulden, N.; Gould, R. O.; Taylor, P.; Yellowlees, L. J.; Welch, A. J. *J. Chem. Soc., Dalton Trans.* **1991**, 3317.

(25) Hodson, B. E.; McGrath, T. D.; Stone, F. G. A. *Organometallics* **2005**, *24*, 3386.

exchange involved in the formation of compounds **2** from compounds **1** and with the metal center identities in the formulas given here.

Extending the synthetic methodology for the deliberate synthesis of compounds **3** from compounds **2**, it was of interest to establish whether the addition of ligands other than CO could effect a similar transformation. Thus, 1 equiv of PEt_3 was added to a CH_2Cl_2 solution of compound **2b**, immediately forming $[N(PPh_3)_2][1,3\text{-}\{Re(CO)_3(PEt_3)\}\text{-}3\text{-}(\mu\text{-}H)\text{-}1,1\text{-}(CO)_2\text{-}2\text{-}Ph\text{-}closo\text{-}1,2\text{-}RhCB_9H_8]$ (**4**). This reagent combination was chosen so that the additional spectroscopic information available from the presence of ^{31}P and ^{103}Rh nuclei would assist in confirming product identity. Compound **4** was characterized by the data in Tables 1−3. In the $^{11}B\{^1H\}$ NMR spectrum, it was immediately evident that an analogue of compounds **3** was formed, with a 1:1:2:1:2:2 intensity pattern confirming mirror symmetry in the product and the chemical shifts being very close to those of **3b**. The $^{31}P\{^1H\}$ NMR spectrum showed (in addition to the signal for the cation) only a singlet at δ 11.4, further confirming that the phosphine was attached to Re and not to Rh. A broad quartet resonance for the B−H⇀Rh proton (δ −7.37) in the ^1H NMR spectrum is again very close to the corresponding data for **3b**. In the CO region of the $^{13}C\{^1H\}$ NMR spectrum, a singlet and two doublets are seen at δ 201.7, 199.3, and 189.7, in the apparent ratio 1:2:2, respectively. The first two of these are assigned to the Re-bound ligands, with the peak at δ 199.3 showing a small, *cis* J(PC) value of 7 Hz, while the third, Rh-bound CO group (δ 189.7) retains a typical J(RhC) coupling of 60 Hz. On the basis of these data alone, it cannot be said whether the phosphine lies *trans* to the Rh−Re bond or to the B−H⇀Re bridge. Although the latter isomer is shown in Chart 1, the former one may be correct: unfortunately, diffraction-quality crystals were not available to distinguish between these two possibilities.

An observation that is interesting alongside the formation of compound **4** was the occasional isolation of the species $[N(PPh_3)_2][1,3\text{-}\{Re(CO)_3(NH_2C_6H_4Me\text{-}1,4)\}\text{-}3\text{-}(\mu\text{-}H)\text{-}1,1\text{-}(CO)_2\text{-}2\text{-}Ph\text{-}closo\text{-}IrCB_9H_8]$ (**5**) during the synthesis of compound **2a**, when using $[IrCl(CO)_2(NH_2C_6H_4Me\text{-}1,4)]$ as the iridium source. The complex **5** apparently was preferred—indeed, was the only Re−Ir metallacarborane isolated—when this reaction was carried out at too low a dilution; a manganese analogue of compound **5** was nevertheless not observed under similar conditions. Compound **5** is also obtained by direct addition of $NH_2C_6H_4$-Me-1,4 to **2a** in CH_2Cl_2. Upon storage in solution for many weeks, compound **5** appeared very slowly to convert to a mixture of **2a** and **3a** in approximately equal proportions, as determined by ^{11}B NMR spectroscopy. Although $[IrCl(CO)_2$-$(NH_2C_6H_4Me\text{-}1,4)]$ was the initial reagent of choice in the synthesis of compound **2a**,[18] inferior yields and the possibility of the undesirable side reaction forming **5** led us to prefer $[N(PPh_3)_2][IrCl_2(CO)_2]$ for preparing **2a**.

Data characterizing **5** are listed in Tables 1−3, and it is immediately apparent from the NMR data that, unlike the ostensibly analogous compounds **3** and **4**, compound **5** lacks mirror symmetry. Thus, the $^{11}B\{^1H\}$ NMR spectrum consists of seven signals in the ratio 1:1:2:1:1:1:2 (the integral-2 peaks being coincidences), while the $^{13}C\{^1H\}$ NMR spectrum displays five separate CO resonances. Peaks attributable to the amino ligand are also seen in typical positions in the $^{13}C\{^1H\}$ and ^1H NMR spectra with, notably, the prochiral NH_2 protons giving rise to two signals (δ 5.42, 4.41), also in keeping with the molecular asymmetry. The latter spectrum also shows a very broad, quartet resonance at δ −5.43 (J(BH) ≈ 120 Hz) due to the sole B−H⇀Re linkage.

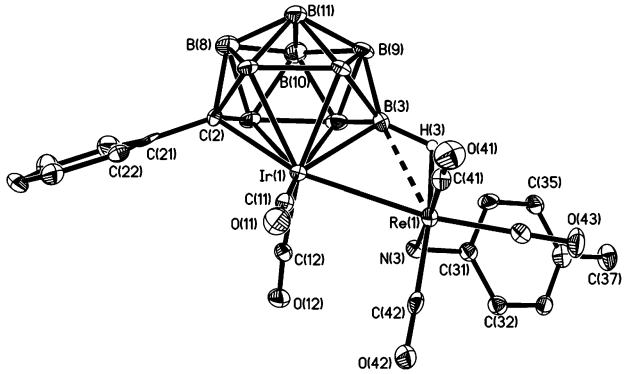

Figure 3. Structure of the anion of **5** showing the crystallographic labeling scheme. Selected distances (Å) and angles (deg) are as follows: Ir(1)−Re(1) 2.8801(3), Ir(1)−C(11) 1.884(6), Ir(1)−C(12) 1.891(6), Ir(1)−C(2) 2.175(5), Ir(1)−B(3) 2.108(6), Ir(1)−B(4) 2.450(6), Ir(1)−B(5) 2.475(7), Ir(1)−B(6) 2.399(6), Ir(1)−B(7) 2.386(6), Re(1)···B(3) 2.360(7), Re(1)−N(3) 2.262(4), Re(1)−C(41) 1.925(7), Re(1)−C(42) 1.901(6), Re(1)−C(43) 1.908(6); C(2)−Ir(1)−Re(1) 164.14(13), N(3)−Re(1)−Ir(1) 86.13(11).

An X-ray diffraction study on **5** (Figure 3) confirmed the asymmetric nature of its anion. A direct Ir−Re bond is present (Ir(1)−Re(1) is 2.8801(3) Å) and the B−H⇀Re bridge is comparable with that in (**3a** and) **3b** (Re(1)···B(3) = 2.360(7), Re(1)−H(3) = 1.66(3) Å). Aside from these features and the $NH_2C_6H_4Me$-1,4 moiety lying off the mirror plane, as expected, the structure is essentially straightforward. The reason for the different location of the $NH_2C_6H_4Me$-1,4 ligand in **5** versus the site of the PEt_3 group in **4** is not clear, but may be related to steric or electronic differences between the two ligands.

Conclusion

The formation of compounds **2** involves the insertion of one {metal−ligand} fragment into the closo cluster of the precursors **1**, with extrusion of the other {metal−ligand} moiety, formerly a cluster vertex, to afford the observed products. This process is apparently without precedent and is facile, occurring readily at ambient temperatures. Compounds **2** themselves react further upon ligand addition to afford the complexes exemplified by compounds **3**−**5**, an observation that may be much exploited in the future by the addition to **2** of other ligands that can potentially be activated by the two adjacent metal centers present. There may also be other, as yet undetected, products or intermediates present in all of these reactions, and their identification may shed light on the processes taking place. Clearly there is much further scope within this area, exploiting other combinations of {metal−ligand} fragments and by employing the many other new monocarboranes that have recently become available.[26] The anions of compounds **2** and **3**, since they retain a negative charge, are also potentially

(26) (a) Brellochs, B. In *Contemporary Boron Chemistry*; Davidson, M. G., Hughes, A. K., Marder, T. B., Wade, K., Eds.; Royal Society of Chemistry: Cambridge, U.K., 2000; p 212. (b) Franken, A.; Kilner, C. A.; Thornton-Pett, M.; Kennedy, J. D. *Collect. Czech. Chem. Commun.* **2002**, *67*, 869. (c) Jelínek, T.; Thornton-Pett, M.; Kennedy, J. D. *Collect. Czech. Chem. Commun.* **2002**, *67*, 1035. (d) Stíbr, B.; Tok, O. L.; Milius, W.; Bakardjiev, M.; Holub, J.; Hnyk, D.; Wrackmeyer, B. *Angew. Chem., Int. Ed.* **2002**, *41*, 2126. (e) Stíbr, B. *Pure Appl. Chem.* **2003**, *75*, 1295. (f) Brellochs, B.; Backovsky, J.; Stíbr, B.; Jelínek, T.; Holub, J.; Bakardjiev, M.; Hnyk, D.; Hofmann, M.; Císarová, I.; Wrackmeyer, B. *Eur. J. Inorg. Chem.* **2004**, 3605.

Table 4. Crystallographic Data for 2b, 3b, and 5

	2b	**3b**	**5·CH_2Cl_2**[a]
formula	$C_{48}H_{44}B_9NO_5P_2ReRh$	$C_{49}H_{44}B_9NO_6P_2ReRh$	$C_{63}H_{63}B_9Cl_2IrN_2O_5P_2Re$
fw	1163.18	1191.19	1536.68
space group	$P\bar{1}$	$P2_1/c$	$P\bar{1}$
a, Å	10.2229(19)	10.295(2)	11.2164(3)
b, Å	14.716(3)	28.103(5)	15.8298(5)
c, Å	17.344(3)	17.398(4)	18.7704(6)
α, deg	105.489(7)	90	80.508(2)
β, deg	102.955(8)	99.739(8)	75.686(2)
γ, deg	94.604(8)	90	79.363(2)
V, Å^3	2423.1(8)	4961.2(19)	3148.80(16)
Z	2	4	2
ρ_{calcd}, g cm^{-3}	1.594	1.595	1.621
μ(Mo Kα), mm^{-1}	2.949	2.884	4.218
no. of rflns measd	49 075	72 385	51 440
no. of indep rflns	15 374	15 978	15 287
R_{int}	0.0419	0.0488	0.0844
wR_2, R_1[b] (all data)	0.0721, 0.0397	0.0579, 0.0449	0.0873, 0.0831
wR_2, R_1 (obsd[c] data)	0.0680, 0.0304	0.0554, 0.0289	0.0745, 0.0450

[a] The crystals contained an unidentified solvate (see text) in addition to one molecule of CH_2Cl_2. The formula and the values for fw, ρ_{calc}, and μ given here ignore the presence of this unknown solvate. [b] $wR_2 = [\sum\{w(F_o^2 - F_c^2)^2\}/\sum w(F_o^2)^2]^{1/2}$; $R_1 = \sum||F_o| - |F_c||/\sum|F_o|$. [c] $F_o > 4\sigma(F_o)$.

suitable substrates for reaction with a further transition metal cation. Such reactions are the subject of the following paper.[22]

Experimental Section

General Considerations. All reactions were performed under an atmosphere of dry, oxygen-free dinitrogen using standard Schlenk-line techniques. Solvents were stored over and freshly distilled from appropriate drying agents prior to use. Petroleum ether here refers to that fraction of boiling point 40−60 °C. Chromatography columns (typically ca. 15 cm in length and ca. 2 cm in diameter) were packed with silica gel (Acros, 60−200 mesh). Filtrations through Celite typically employed a plug ca. 5 cm in depth. Elemental analyses were performed by Atlantic Microlab, Inc., Norcross, GA, on crystalline or microcrystalline samples that had been dried overnight in vacuo. On occasion residual solvent remained after drying, its presence and approximate proportion confirmed by integrated ^{1}H NMR spectroscopy, and this was factored into the calculated microanalysis data. NMR spectra were recorded at the following frequencies (MHz): ^{1}H, 360.1; ^{13}C, 90.6; ^{11}B, 115.5; and ^{31}P, 145.8. Complexes **1a**,[19] **1b**,[17] and [IrCl(CO)$_2$(NH$_2$C$_6$H$_4$Me-1,4)][27] were prepared by literature methods. The reagent [N(PPh$_3$)$_2$][IrCl$_2$(CO)$_2$][28] was prepared from [Ir$_2$Cl$_2$(η^2-C$_8$H$_{14}$)$_4$][29] and used without purification: the presence of traces[28] of [IrCl(CO)$_2$]$_n$ did not affect reactions, as the latter reagent also reacted with **1b** to form **2a**. All other materials were used as received.

Synthesis of [N(PPh$_3$)$_2$][1,3,6-{M(CO)$_3$}-3,6-(μ-H)$_2$-1,1-(CO)$_2$-2-Ph-*closo*-1,2-M′CB$_9$H$_7$] (M = Re, Mn; M′ = Ir, Rh). (i) (a) In a typical reaction, a solution of complex **1b** (0.200 g, 0.18 mmol) and [N(PPh$_3$)$_2$][IrCl$_2$(CO)$_2$] (0.155 g, 0.18 mmol) in CH_2Cl_2 (20 mL) was prepared, and to this was added Tl[PF$_6$] (0.064 g, 0.18 mmol). The resulting mixture was stirred for 4 h. After filtration (Celite), the filtrate was evaporated in vacuo and the residue subjected to column chromatography. Elution with CH_2Cl_2−petroleum ether (3:1) gave a bright yellow band, from which yellow, microcrystalline [N(PPh$_3$)$_2$][1,3,6-{Re(CO)$_3$}-3,6-(μ-H)$_2$-1,1-(CO)$_2$-2-Ph-*closo*-1,2-IrCB$_9$H$_7$] (**2a**; 0.138 g) was obtained after removal of solvent in vacuo. (b) Alternatively, compound **1b** (0.200 g, 0.18 mmol), [IrCl(CO)$_2$(NH$_2$C$_6$H$_4$Me-1,4)] (0.071 g, 0.18 mmol), and Tl[PF$_6$] (0.064 g, 0.18 mmol) stirred overnight in CH_2Cl_2 (25 mL) gave **2a** (0.103 g, 47%) by an analogous procedure and workup. On occasion, a similar procedure instead afforded [N(PPh$_3$)$_2$][1,3-{Re(CO)$_3$(NH$_2$C$_6$H$_4$Me-1,4)}-3-(μ-H)-1,1-(CO)$_2$-2-Ph-*closo*-1,2-IrCB$_9$H$_8$] (**5**) as the only isolated metallacarborane product. This was apparently a consequence of the reaction being performed at too low a dilution.

(ii) By a procedure similar to (i) (a), a mixture of compound **1b** (0.870 g, 0.77 mmol), [Rh$_2$(μ-Cl)$_2$(CO)$_4$] (0.150 g, 0.39 mmol), and Tl[PF$_6$] (0.270 g, 0.77 mmol) was stirred in CH_2Cl_2 (30 mL) for 2 h, after which workup as above gave [N(PPh$_3$)$_2$][1,3,6-{Re(CO)$_3$}-3,6-(μ-H)$_2$-1,1-(CO)$_2$-2-Ph-*closo*-1,2-RhCB$_9$H$_7$] (**2b**; 0.495 g) as an orange-yellow microcrystalline solid.

(iii) Compound **1a** (0.150 g, 0.15 mmol) and [IrCl(CO)$_2$(NH$_2$C$_6$H$_4$Me-1,4)] (0.058 g, 0.15 mmol) were dissolved in CH_2Cl_2 (10 mL) at −78 °C, and the mixture was warmed to room temperature with vigorous stirring. After 30 min, the reaction mixture was cooled to 0 °C and volatile materials were removed in vacuo. The residue was taken up in CH_2Cl_2−petroleum ether (2:1, 2 mL) and applied to a chromatography column that was maintained at 0 °C. Elution with the same solvent mixture gave a dark red band that was collected at 0 °C and evaporated in vacuo to give [N(PPh$_3$)$_2$][1,3,6-{Mn(CO)$_3$}-3,6-(μ-H)$_2$-1,1-(CO)$_2$-2-Ph-*closo*-1,2-IrCB$_9$H$_7$] (**2c**) (0.054 g) as a dark red, microcrystalline solid.

(iv) Similarly, compound **1a** (0.150 g, 0.15 mmol) and [Rh$_2$(μ-Cl)$_2$(CO)$_4$] (0.029 g, 0.075 mmol) gave [N(PPh$_3$)$_2$][1,3,6-{Mn(CO)$_3$}-3,6-(μ-H)$_2$-1,1-(CO)$_2$-2-Ph-*closo*-1,2-RhCB$_9$H$_7$] (**2d**) (0.049 g) as dark red-orange microcrystals.

Synthesis of [N(PPh$_3$)$_2$][1,3-{M(CO)$_4$}-3-(μ-H)-1,1-(CO)$_2$-2-Ph-*closo*-1,2-M′CB$_9$H$_8$] (M = Re, Mn; M′ = Ir, Rh). All four of compounds **3** were obtained in almost quantitative yield from the corresponding compounds **2** by passing CO through a CH_2Cl_2 solution (15 mL; ca. 50 μmol reaction scale) with stirring at room temperature for 1 h (**3a**, **3b**) or 20 min (**3c**, **3d**) until IR and ^{11}B-{^{1}H} NMR spectra indicated that conversion was complete. Thereafter the solution was evaporated and the product purified by passing it down a short (5 cm) chromatography column, elution with CH_2Cl_2−petroleum ether (3:1) affording a single yellow band, which was collected and evaporated to dryness to give the appropriate compound **3**.

Compounds **3** could also be obtained by simply stirring a CH_2Cl_2 solution of the corresponding compound **2** at room temperature for several days, with spectroscopic monitoring and chromatographic workup. However, this route afforded the products in poorer yield and inferior purity.

Synthesis of [N(PPh$_3$)$_2$][1,3-{Re(CO)$_3$(PEt$_3$)}-3-(μ-H)-1,1-(CO)$_2$-2-Ph-*closo*-1,2-RhCB$_9$H$_8$]. A sample of compound **2b** (0.050 g, 0.04 mmol) was dissolved in CH_2Cl_2 (5 mL), and to the

(27) Klabunde, U. *Inorg. Synth.* **1974**, *15*, 82.
(28) Roberto, D.; Cariati, E.; Psaro, R.; Ugo, R. *Organometallics* **1994**, *13*, 4227.
(29) (a) Herde, J. L.; Lambert, J. C.; Senoff, C. V. *Inorg. Synth.* **1974**, *15*, 18. (b) van der Ent, A.; Onderdelinden, A. L. *Inorg. Synth.* **1990**, *28*, 90.

vigorously stirred solution was added PEt_3 (6.5 μL, 0.0052 g, 0.04 mmol). The mixture rapidly became lighter yellow and after 1 h was evaporated. Column chromatography of the residue, eluting with CH_2Cl_2, afforded a yellow band, which was collected and evaporated in vacuo to yield yellow microcrystals of $[N(PPh_3)_2]$-[1,3-{$Re(CO)_3(PEt_3)$}-3-(μ-H)-1,1-$(CO)_2$-2-Ph-*closo*-1,2-$RhCB_9H_8$] (**4**; 0.049 g).

Synthesis of $[N(PPh_3)_2]$[1,3-{$Re(CO)_3(NH_2C_6H_4Me$-1,4)}-3-(μ-H)-1,1-$(CO)_2$-2-Ph-*closo*-1,2-$IrCB_9H_8$]. Similar to the synthesis of **4**, compound **2a** (0.050 g, 0.04 mmol) and $NH_2C_6H_4Me$-1,4 (0.0045 g, 0.04 mmol) gave $[N(PPh_3)_2]$[1,3-{$Re(CO)_3(NH_2C_6H_4$-Me-1,4)}-3-(μ-H)-1,1-$(CO)_2$-2-Ph-*closo*-1,2-$IrCB_9H_8$] (**5**; 0.043 g) as very pale yellow microcrystals.

X-ray Crystallographic Structure Determinations. Experimental data for **2b**, **3b**, and **5** are presented in Table 4. X-ray intensity data were collected at 110(2) K on a Bruker-Nonius X8 APEX CCD area-detector diffractometer using Mo Kα X-radiation. Several sets of narrow data "frames" were collected at different values of θ, for various initial values of ϕ and ω, using 0.5° increments of ϕ or ω. The data frames were integrated using SAINT;[30] the substantial redundancy in data allowed an empirical absorption correction (SADABS)[30] to be applied, based on multiple measurements of equivalent reflections.

All structures were solved using conventional direct methods[30,31] and refined by full-matrix least-squares on all F^2 data using SHELXTL version 6.12,[31] with anisotropic thermal parameters assigned to all non-H atoms. The locations of the cage-carbon atoms were verified by examination of the appropriate internuclear distances and the magnitudes of their isotropic thermal displacement parameters. Cluster BH hydrogens, apart from H(3) in **5**, were allowed positional refinement; all other H atoms were set riding in calculated positions. All hydrogens had fixed isotropic thermal parameters defined as $U_{iso}(H) = 1.2U_{iso}(parent)$, or $U_{iso}(H) = 1.5U_{iso}(parent)$ for methyl groups.

The crystal studied for compound **5** was of only modest quality, and some difficulty was experienced in modeling the solvates that cocrystallized alongside the compound. Of these solvates, one was a molecule of CH_2Cl_2 that was ordered and treated without problems. However, there was also a second solvated volume that apparently contained highly disordered toluene and/or pentane and/or partial CH_2Cl_2 molecules. These were modeled as 14 partial carbon atoms with refining occupancies and isotropic thermal parameters. No attempt was made to include hydrogen atoms.

Acknowledgment. We thank the Robert A. Welch Foundation for support (Grant AA-0006). The Bruker-Nonius X8 APEX diffractometer was purchased with funds received from the National Science Foundation Major Instrumentation Program (Grant CHE-0321214).

Supporting Information Available: Full details of the crystal structure analyses in CIF format, including data for compounds **3a**, **3c**, and **3d**. This material is available free of charge via the Internet at http://pubs.acs.org.

OM060417Z

(30) *APEX 2*, version 1.0; Bruker AXS: Madison, WI, 2003−2004.
(31) *SHELXTL*, version 6.12; Bruker AXS: Madison, WI, 2001.